Reduced order modelling of vibroelastic response of a hydrofoil in homogeneous isotropic turbulence

Konstantinos Tsigklifis (1,2), Marcus Wong (1), Steven De Candia (1), Paul Dylejko (1), Paul Croaker (1) and Alex Skvortsov (1)

(1) Maritime Division, Defence Science and Technology Group, Melbourne, VIC 3207, Australia
(2) YTEK Pty Ltd, Level 1, 231 High St, Ashburton, VIC 3147, Australia

ABSTRACT
The paper deals with a reduced order analytical model of the vibration response of a NACA0015 cantilevered hydrofoil excited by honeycomb-generated turbulence. The statistical stochastic excitation model employs strip theory with the intensity and the integral length-scale of the turbulence being the input parameters. The structural response is calculated as the product of the total hydrodynamic response function with the frequency spectrum of the space-time velocity correlation function. The total hydrodynamic response is represented by the combination of Sears' model of unsteady hydrodynamic gust combined with Theodorsen's theory for the lift and moment due to the heaving and pitching motion of the strip coupled with Euler-Bernoulli and torsional equations of the cantilevered hydrofoil motion. The comparison of the predicted structural velocity spectra with available experimental results shows good agreement for the first bending mode but overpredicts the amplitude at higher frequencies. Finally, a finite/boundary element model developed using COMSOL Multiphysics, provides further cross-verification with the aim of understanding some of the limitations of the simplified analytical model.

1 INTRODUCTION
The study of the hydroelastic behaviour of a flexible lifting surface is important for the design of maritime vessels (D' Ubaldo et al., 2021, Jang et al., 2020). The optimally designed lifting surface usually operates under relatively small angles of incidence to avoid flow separation, excessive noise and material damage. Previous studies have focused on the hydrostability characteristics of the flexible lifting surface (Dowell, 2015, Ducoin and Young, 2013), investigating the critical operating conditions where divergence or flutter instabilities set in, causing a failure of the hydroelastic system. Of equal importance, however, is the lifting surface's vibration response due to excitation by the surrounding fluid. Excitation mechanisms include the leading edge interacting with the free stream turbulent vortices (Chae et al., 2016, Lelong et al., 2018), stochastic forcing by the turbulent boundary layer along the surface or from its separation (Ducoin et al., 2012, Ducoin and Young, 2013). Such interactions can lead to unwanted noise generation, transmission to other platform components and high-cycle fatigue failure.

Experimental measurements of the vibration response of a cantilevered NACA0015 hydrofoil of Polyacetate(POM) material with chord $c = 0.1$m and span $L = 0.191$m, interacting with the free stream turbulent vortices generated by an upstream honeycomb (see Figure 1), were conducted at the French Naval Academy Research Institute (Chae et al., 2016, Lelong et al., 2016,2018). The objective of the present study is to detail the development of a stochastic model to simulate the vibration response of this cantilevered hydrofoil due to the interaction of its leading edge with the free stream vortices of an unconfined flow. Validation of the analytical model is made by comparing with the corresponding experimental vibration spectra(Lelong et al., 2016,2018) and results from Finite Element (FE) / Boundary Element (BE) models.

2 MATHEMATICAL FRAMEWORK

2.1 Hydroelastic Response
The effect of hydrofoil elasticity on the frequency spectrum of the structural response is studied by incorporating the hydrodynamic gust response function into the hydroelastic response function (Dowell,2015, Blake and Maga, 1975). The hydroelastic response function is built based on the equation of motion of a typical section, or strip of the hydrofoil shown in Figure 2. The parameters used in the hydroelastic response function includes the mass, mass moment of inertia, structural damping as well as linear and torsional stiffness of the strip due to heaving and pitching of the elastic axis. Coupling of the structural inertia is also considered when the centre of mass does not coincide with the elastic axis.

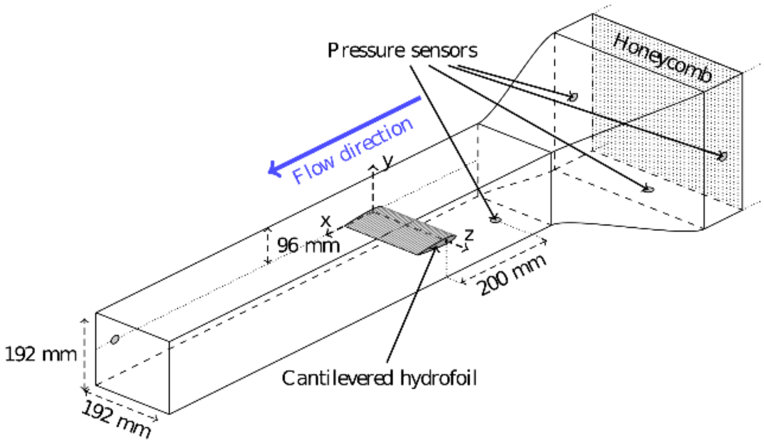

Figure 1: Experimental setup of a cantilevered hydrofoil mounted horizontally inside the water channel (reproduced from Chae et al. (2016))

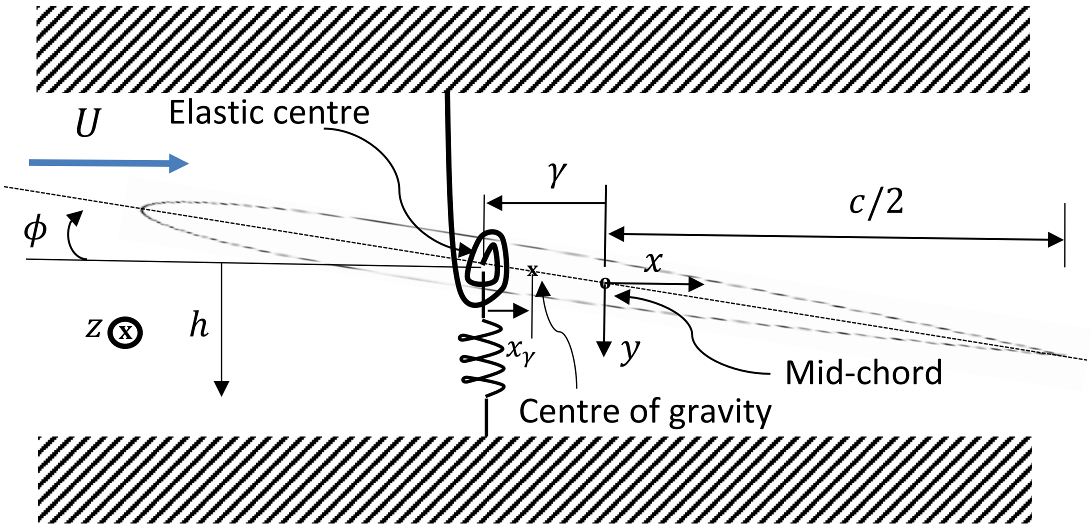

Figure 2: Geometry of a hydrofoil strip

The Euler-Bernoulli and the torsional equations of the beam (Rao, 2007) characterise the bending and torsional vibrations of the hydrofoil. The Euler-Bernoulli model is valid for the low order structural bending modes observed in the experimental results. The hydrofoil aspect ratio and frequency range of interest in this work is low, it is therefore assumed that the chordwise bending modes of the plate do not significantly contribute. The simplest analytical models that quantify the unsteady lift and moment of a hydrofoil using unsteady 2D hydrofoil theory, are the sinusoidal motion of the hydrofoil section at heaving and pitching in steady flow, namely the Theodorsen's model, and the interaction of the leading edge of a rigid hydrofoil with a sinusoidal gust, that is the Sears' model. The overall response emerges from the superposition of the responses of the two linear models. The forcing terms in the two equations are the lift and moments imposed at a section of the hydrofoil due to the gust velocity (Sears, 1941) and the lift and moments imposed by the fluid due to the heaving (bending) and pitching (torsion) of the hydrofoil section (Theodorsen, 1935). The bending and torsional equations that characterise each strip of the hydrofoil and the boundary conditions, are

$$\rho_s A\frac{\partial^2 h}{\partial t^2} + S_\phi\frac{\partial^2 \phi}{\partial t^2} + (D_h + D_\alpha)\frac{\partial h}{\partial t} + EI\frac{\partial^4 h}{\partial z^4} = L_G + L_{HP} = -\frac{\partial C_l}{\partial \phi}\rho_l\frac{c}{2}US(s)\widehat{W}\,e^{-i\omega t} - \frac{\pi\rho_l\frac{c^2}{4}}{M_c}\left(\frac{\partial^2 h}{\partial t^2} + U\frac{\partial \phi}{\partial t} - \frac{c}{2}\gamma\frac{\partial^2\phi}{\partial t^2}\right) - \pi\rho_l cUT(s)\left(\frac{\vartheta h}{\vartheta t} + U\phi + \frac{c}{2}\left(\frac{1}{2}-\gamma\right)\frac{\partial\phi}{\partial t}\right) \quad (1)$$

$$I_0\frac{\partial^2\phi}{\partial t^2} + S_\phi\frac{\partial^2 h}{\partial t^2} + D_\phi\frac{\partial\phi}{\partial t} - GJ_T\frac{\partial^2\phi}{\partial z^2} = M_G + M_{HP} = \frac{\partial C_l}{\partial\phi}\rho_l\frac{c^2}{4}\left(\frac{1}{2}+\gamma\right)US(s)\widehat{W}\,e^{-i\omega t} - \frac{\pi\rho_l\frac{c^2}{4}}{M_c}\left(-\frac{c}{2}\gamma\frac{\partial^2 h}{\partial t^2} + \frac{c^2}{4}\left(\frac{1}{8}+\gamma^2\right)\frac{\partial^2\phi}{\partial t^2} + \left(\frac{1}{2}-\gamma\right)U\frac{c}{2}\frac{\partial\phi}{\partial t}\right) + \pi\rho_l\frac{c^2}{2}\left(\frac{1}{2}+\gamma\right)UT(s)\left(\frac{\vartheta h}{\vartheta t} + U\phi + \frac{c}{2}\left(\frac{1}{2}-\gamma\right)\frac{\partial\phi}{\partial t}\right) \quad (2)$$

with boundary conditions

$$\frac{\partial h}{\partial z}(z=0,t)=0,\ \ h(z=0,t)=0,\ \ \frac{\partial^2 h}{\partial z^2}(z=L,t)=0,\ \ \frac{\partial^3 h}{\partial z^3}(z=L,t)=0 \tag{3a,b,c,d}$$

$$\phi(z=0,t)=0,\ \ \frac{\partial \phi}{\partial z}(z=L,t)=0 \tag{4a,b}$$

In the above equations, $h(z,t)$ is the vertical displacement of the elastic axis of the strip (positive downwards), $\phi(z,t)$ is the angular displacement (positive clockwise) of the elastic axis positioned $\frac{\gamma c}{2}$ from the mid-chord of the strip, considered positive towards the trailing edge of the hydrofoil with c and L the strip chord and the span of the hydrofoil, respectively. The density of the hydrofoil material is assigned by ρ_s, A is the cross sectional area and I_0 is the mass moment of inertia per unit span. D_h, D_ϕ is the damping of the structural vibration in bending and torsion due to the fluid viscosity and D_α is the damping due to the acoustic radiation (Blake and Maga, 1975), which is considered negligible for the present study. EI is the flexural rigidity and GJ_T is the torsional rigidity. $S_\phi = \frac{x_\gamma \rho_s A c}{2}$ is the moment of the mass per unit span due to the offset $\frac{x_\gamma c}{2}$ of the centre of mass from the elastic centre. ρ_l is the fluid density, U is the free stream velocity of the strip and $T(s)$ and $S(s)$ are Theodorsen's (Theodorsen, 1935) and Sears' functions (Glegg and Devenport, 2017), respectively. $s=\omega c/(2U)$ is the non-dimensional (reduced) frequency of the wake which coincides to that of the unsteady gust and $\widehat{W}$ the magnitude of the sinusoidal gust velocity. $\frac{\partial C_l}{\partial \phi}$ is the local lift curve slope of the strip which for an infinite span hydrofoil of infinitesimal thickness is $\left(\frac{\partial C_l}{\partial \phi}\right)_\infty = 2\pi$. The experimental results (Chae et al. 2016, Lelong et al. 2016, 2018) were obtained for a cantilevered hydrofoil whose tip was constrained by a wall minimizing the tip loss and thus $\frac{\partial C_l}{\partial \phi} \approx \left(\frac{\partial C_l}{\partial \phi}\right)_\infty$ was assumed. An empirical correction to the two-dimensional lift curve-slope due to the finite thickness of the strip section was also used (Houghton and Carpenter, 2003)

$$\left(\frac{\partial C_l}{\partial \phi}\right)_\infty = 1.8\pi\left(1+0.8\frac{t_{max}}{c}\right) \tag{5}$$

with t_{max}, the maximum thickness of the section.

In Theodorsen's model, the added mass has been obtained for an incompressible potential flow. To account for a modification (decrease) of the added mass due to the increase of the disturbance frequency, the following correction factor M_c was used in equations (1) and (2)

$$M_c = \frac{1}{2}\left[1 + k_a c\sqrt{\left(\frac{k_n}{k_a}\right)^2 - 1}\right],\ k_a = \frac{\omega}{c_\infty},\ k_n \approx \frac{(2n-1)\pi}{2L}, n>1 \tag{6a,b,c}$$

which is valid for $1 < k_n c < 4.4$ and $\frac{k_a}{k_n} \ll 1$, with k_a referring to the acoustic wavenumber and n the structural mode number. This theoretical formula was obtained by (Blake, 1974) when calculating the pressure radiation of a vibrating free-free unbaffled beam. Initially, the analytical eigenfrequencies of the bending modes of the beam with the geometric and elastic properties of the hydrofoil in water for correction factor $M_c = 1$ are calculated from $\omega_n = (k_n L)^2\left(\frac{EI}{\left(\rho_s A + \frac{\pi \rho_l c^2}{4M_c}\right)L^4}\right)^{1/2}, n \geq 1$. For given frequency ω, the bending mode number of vibration at that frequency is known and using equations 6(b),(c) in 6(a), the new correction factor M_c is calculated. The latter one is used to find the new eigenfrequencies in water from the above equation and the procedure continues until convergence of the correction factor $\mathrm{M_c}$ in about 1-3 iterations.

Applying the wave-type decomposition, $h(z,t) = \hat{h}(z)e^{-\mathrm{i}\omega t}$, $\phi(z,t) = \hat{\phi}(z)e^{-\mathrm{i}\omega t}$ to equations (1)-(4), a system of ordinary differential equations with respect to the spanwise direction z is obtained:

$$\underline{\underline{A}} \begin{Bmatrix} \frac{\hat{h}(z)}{\widehat{W}} \\ \frac{\hat{\phi}(z)}{\widehat{W}} \end{Bmatrix} = \underline{b} \tag{7}$$

where the vector $\underline{b}$ involves the lift and moment due to the unsteady hydrodynamic gust. The two boundary conditions for bending and one boundary condition for torsion applied at each end of the beam, supplement the system of equations. Finally, a second order central finite difference scheme was applied for the discretization of the spatial derivatives of the bending and torsional equations of the above system which produces a $(M+1)\times(M+1)$ algebraic linear system of equations with M the number of strips used for the hydrofoil discretization.

The total lift hydrodynamic response function H_{NN}^{α} of strip α, is given as the sum of the lift hydrodynamic gust response due to the up-wash velocity (normal velocity fluctuations on the hydrofoil), HL_{NN}^{α} and the lift hydroelastic response due to the heaving and pitching motion of the section, HL_{HP}^{α}

$$H_{NN}^{\alpha}(\omega) = HL_{NN}^{\alpha}(\omega) + HL_{HP}^{\alpha}(\omega) = -\frac{\partial C_l}{\partial \phi}\rho_l \frac{c}{2} US(s)\delta z - \frac{\pi\rho_l \frac{c^2}{4}}{M_c}\left(-\omega^2 \frac{\hat{h}}{\hat{W}} - \mathrm{i}\omega U \frac{\hat{\phi}}{\hat{W}} + \frac{c}{2}\gamma\omega^2 \frac{\hat{\phi}}{\hat{W}}\right)\delta z - \pi\rho_l c U T(s)\left(-\mathrm{i}\omega \frac{\hat{h}}{\hat{W}} + U\frac{\hat{\phi}}{\hat{W}} - \frac{c}{2}\left(\frac{1}{2}-\gamma\right)\mathrm{i}\omega \frac{\hat{\phi}}{\hat{W}}\right)\delta z \quad (8)$$

with δz the length of the strip. Similarly, the structural vertical velocity response of strip α is given by

$$H_V^{\alpha}(\omega) = -\frac{\mathrm{i}\omega \frac{\hat{h}}{\hat{W}}\delta z}{L} \quad (9)$$

2.2 Turbulence Ingestion

The correlation method (Sevik, 1974, Jiang et al., 1991) for the turbulence ingestion of the elastic hydrofoil is implemented and combined with the above structural vertical velocity response function. The hydrofoil is discretised into chordwise strips along the span. The frequency spectrum of the correlation function of the lift between two strips α and β due to the normal velocity fluctuations on these strips , $\Psi_{NN}^{\alpha\beta}(\omega)$ is defined as

$$\Psi_{NN}^{\alpha\beta}(\omega) = \frac{1}{2\pi}\int_{-\infty}^{+\infty} P_{NN}^{\alpha\beta}(\tau)\, e^{\mathrm{i}\omega\tau}\, d\tau \quad (10)$$

with $P_{NN}^{\alpha\beta}(\tau)$ being the correlation function of the lift and τ the time delay. The frequency spectrum of the correlation function of the lift of the hydrofoil is related to the Fourier transform of the space-time correlation function of the normal velocities fluctuations on the hydrofoils, $S_{NN}^{\alpha\beta}(\omega)$ as

$$\Psi_{NN}(\omega) = \sum_{\alpha=1}^{M}\sum_{\beta=1}^{M} {H_{NN}^{\alpha}}^{*}(\omega) H_{NN}^{\beta}(\omega) S_{NN}^{\alpha\beta}(\omega) \quad (11)$$

with $H_{NN}^{\alpha}(\omega)$ is given by (8) and $S_{NN}^{\alpha\beta}$ is defined by the Fourier transform of the space-time correlation of the velocity's fluctuations normal to the hydrofoil, $R_{NN}^{\alpha\beta}(\tau)$

$$S_{NN}^{\alpha\beta}(\omega) = 2\pi\int_{-\infty}^{+\infty} R_{NN}^{\alpha\beta}(\tau)\, e^{\mathrm{i}\omega\tau}\, d\tau,\;\; R_{NN}^{\alpha\beta}(\tau) = E\left(u_y^{\alpha}(t)\, u_y^{\beta}(t+\tau)\right) = R_{yy}(r(\tau)) \quad (12a,b)$$

In the above expression, r is the separation distance between strip α and the frozen convected vortices as they pass through strip β on the hydrofoil plane (xz plane). By analogy to equation (11), the frequency spectrum of the correlation function of the structural vertical velocity vibrations of the hydrofoil is given by

$$\Psi_{VV}(\omega) = \sum_{\alpha=1}^{M}\sum_{\beta=1}^{M} H_V^{\alpha *}(\omega) H_V^{\beta}(\omega) S_{NN}^{\alpha\beta}(\omega) \quad (13)$$

with $H_V^{\alpha}(\omega)$ given by (9).

The spatial correlation function for homogeneous isotropic turbulence is defined as (Glegg and Devenport, 2017)

$$R_{ij}(\xi_x, \xi_y, \xi_z) = \overline{u^2}\left[g(r)\delta_{ij} + \frac{f(r)-g(r)}{r^2}\xi_i\xi_j\right] \quad i,j = x,y,z \quad (14)$$

with the separation distance given by

$$r(\tau) = \sqrt{\xi_x^2 + \xi_y^2 + \xi_z^2} = \sqrt{(U_c\tau)^2 + \xi_z^2} = \sqrt{(U_c\tau)^2 + (z^{\beta} - z^{\alpha})^2} \quad (15)$$

where $\overline{u^2}$ is the mean square of the velocity fluctuations, $U_c \sim 0.7U$ the convection velocity of the free stream vortices and ξ_z the Cartesian separation distance in the spanwise direction. Using the Liepmann spectrum the longitudinal $f(r)$ and lateral $g(r)$ correlation coefficient functions are defined, respectively by (Glegg and Devenport, 2017)

$$f(r) = e^{-\frac{r}{\Lambda_f}},\ g(r) = e^{-\frac{r}{\Lambda_f}}\left(1 - \frac{r}{2\Lambda_f}\right) \tag{16a,b}$$

with Λ_f the longitudinal integral lengthscale of turbulence. The space-time correlation function is simplified to

$$R_{NN}^{\alpha\beta}(\tau) = R_{yy}(r(\tau)) = \overline{u^2}g(r) = \overline{u^2}e^{-\frac{r}{\Lambda_f}}\left(1 - \frac{r}{2\Lambda_f}\right) \tag{17}$$

The correlation of the normal velocity fluctuations between two strips is calculated from equation (17) and its frequency spectrum from equation (12) using a standard Gauss integration. The total interval of the integral is set to 20 periods of the considered gust, while the time step is set to 1/30th of the gust period. The results appears to be insensitive to larger intervals or smaller time steps for the frequencies of the gusts considered.

2.3 COMSOL Modelling

In order to validate the analytical model presented, the hydrofoil is modelled using the COMSOL Multiphysics FEM software. The software is capable of coupling the acoustic-structure interaction at the fluid-structure boundary, allowing the effect of the added fluid mass to be captured. To solve the coupled vibroacoustic problem, a hybrid FEM-BEM method was employed (Everstine and Henderson, 1990). The FEM model was used to describe structural domain (hydrofoil) while the BEM was used for the fluid domain. A system of equations is constructed in terms of nodal velocities and sound pressure (Merz et al., 2007). A GMRES iterative solver along with a GCRO-DR preconditioner is used to solve the system of equations. Solid tetrahedral elements are used for both the structure and fluid domains and the final mesh results in the total number of DOFs in the system to be 34996. One major difference between the COMSOL model and the analytical model is that the prediction in equation (7) assumes a freely propagating acoustic field; reflection and wall effects are not captured. Moreover, the near wall effects at the tip of the hydrofoil are also not captured by the analytical model. An eigenfrequency analysis was performed and the first two spanwise bending and torsional mode shapes were extracted.

3 RESULTS AND DISCUSSION

3.1 Resonant Frequencies In Air And Water

The resonant frequencies of the NACA0015 cantilevered hydrofoil in still air and water is considered. The system response predicted by the model is compared with respective experimental results (Lelong et al. (2016)) and modal analysis in COMSOL. Table 1 shows the geometry, material and flow properties used to evaluate the resonant frequencies of the cantilever hydrofoil in both a still and moving flow as well as its structural response when ingesting a homogeneous isotropic turbulent flow. Equation (7) is solved to find the amplitudes of vertical displacements and rotation of each strip. Equation (13), combined with equations (9), (12) and (17), then provides the structural vertical velocity spectra of the cantilevered hydrofoil. For the still air and water case, the velocity of the free stream is set close to zero, with the turbulent velocity fluctuations used as a broadband excitation force. In the results to follow, this approach is termed the ‘correlation method’.

Figure 3(a) and (b) show the resonant frequencies in still air and water, respectively, of the NACA0015 cantilevered hydrofoil. The experimental measurements and predictions from the COMSOL modal analysis are represented by the black dashed and green dotted vertical lines, respectively. The results from the correlation method with and without the modification of the added mass with the disturbance frequency, equation (6), are depicted by the blue dotted and red solid line, respectively. These results show that the added mass correction has a negligible effect on the resonant frequencies in air but a large effect in water for the higher order modes.

Table 1: Geometry, material and flow properties used in the present study

Geometry: NACA0015 cantilevered hydrofoil	
Span, L (m)	0.191
Chord, c (m)	0.1
Thickness, t_{max} (m)	0.15c
Material: POM	
Material density, ρ_s(kg/m^3)	1420
Elastic modulus, E (GPa)	2.9
Poisson ratio, ν	0.35
Type of force: Turbulent velocity fluctuations	
Free stream velocity, U (m/s)	~0,4,5,6
rms of velocity fluctuations, $\sqrt{\overline{u^2}}$ (m/s)	0.02U
Longitudinal Integral lengthscale, Λ_f (m)	0.0022

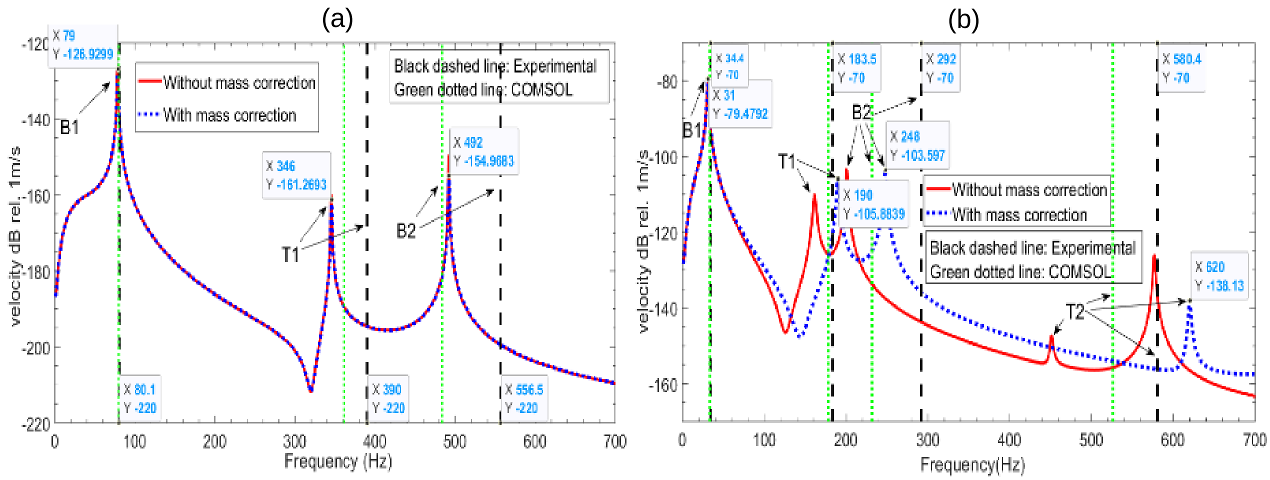

Figure 3: Structural vertical velocity spectra of a NACA0015 cantilevered hydrofoil predicted by the correlation method in still (a) air and (b) water. The green and black vertical lines represent the resonant frequencies predicted by modal analysis with COMSOL and the experimental measurements, respectively. The 1st, 2nd bending (B1, B2) and 1st, 2nd torsional modes (T1, T2) are shown with the arrows.

Table 2: Bending and torsional resonant frequencies in still air and water

Bending resonant frequencies (Hz)						
	Air			**Water**		
	Experiment	**Correlation method**	**COMSOL**	**Experiment**	**Correlation method**	**COMSOL**
1st mode	80.6	79	80.1	34.4	31	33.6
2nd mode	556.5	494	483.3	292	248	231.7
Torsional resonant frequencies (Hz)						
	Air			**Water**		
	Experiment	**Correlation method**	**COMSOL**	**Experiment**	**Correlation method**	**COMSOL**
1st mode	390	346	361.5	183.5	190	178.6
2nd mode	-	-	-	580.4	621	526.1

A summary of the resonant frequencies in still air and water produced by the experiment, the correlation method and the modal analysis in COMSOL appears in Table 2.There are a number of reasons which could lead to discrepancies between the three sets of data. Firstly, the effect of the wall adjacent to the hydrofoil tip is not accounted for by the correlation method; the hydrofoil is assumed to be in free space while in both the experiment and COMSOL model a rigid wall is present. The presence of the wall increases the entrained fluid mass of the cantilever hydrofoil and thus the resonant frequencies are reduced with the effect being more significant for the water case. This was verified by the analysis in COMSOL with and without the presence of the wall. Secondly, there is a non-perfect clamped boundary condition in the experiment and uncertainty in the material properties of the hydrofoil. Thirdly, the correlation method neglects interactions between neighbouring strips, thus overpredicting the effect of the added mass. Finally, the mass correction equation (6) is an approximate one, valid when the acoustic wavelength is much larger than the wavelength of the structural mode.

3.2 Structural Response Due To Turbulence Interaction

The structural response due to turbulence ingestion of a NACA0015 cantilevered hydrofoil immersed in a turbulent flow produced by water flowing through a honeycomb is discussed. Since the longitudinal integral lengthscale of turbulence is an unknown, it is assumed to be $\Lambda_f = 0.0022$ m for the present study. This was determined by matching the numerically obtained maximum PSD of the first bending mode with that of the experimental data at U=4 m/s. The relative turbulence forcing parameters used in the correlation method are given in Table 1. Figure 4(a) shows the structural response due to turbulence ingestion, as expressed by the structural velocity spectra of the NACA0015 cantilevered hydrofoil. Converged solution within 0.3dB was obtained with 150 strips across the whole frequency spectrum. Free stream velocities of $U = 4, 5$ & 6 m/s are represented by blue solid, red dashed dotted and green dotted curves, respectively. The thick lines represent the experimental measurements at 2 degrees angle of flow incidence(Lelong et al., 2018) with the thin lines representing the predictions of the correlation method.

Results obtained using Sears' function are shown to over predict the response of the 1st torsion and 2nd bending modes as well as of the response at the higher frequency range. In addition, some differences observed in the frequency spectrum of the peaks of the second bending mode between the correlation method and the experimental measurements are associated with differences of the resonant frequencies in still water as presented in Figure 3(b). As the flow velocity increases, the experimental results are showing an increase in resonant frequency of approximately 5Hz and 11Hz for the 1st torsional and 2nd bending modes, respectively. On the other hand, the correlation method predicts an increase in the resonant frequency only for the 1st torsional mode of about 1Hz with increasing flow velocity. Despite these differences, as shown in Figure 4(a), the correlation method is able to capture the effect of hydrodynamic damping on the structural response across the flow speeds investigated.

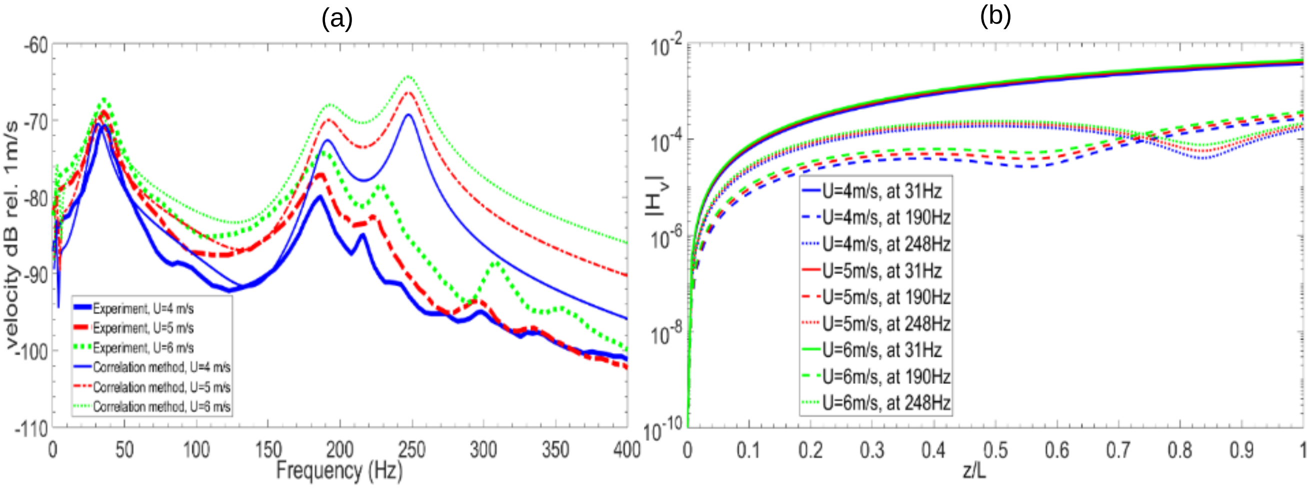

Figure 4: (a) Vertical velocity spectra of hydrofoil (calculation and experiments in water). (b) Magnitude of the vertical velocity response function at the resonance as a function of span location and free stream velocity (water).

Finally, Figure 4(b) shows the spanwise distribution of the magnitude of the structural vertical velocity response function, given by equation (9), at the resonant frequencies of the 1st, 2nd bending (at 31 and 248 Hz, respectively) and 1st torsional (at 190Hz) modes with increasing free stream velocity. It can be seen that the vibration response increases with the free stream velocity, with the largest magnitude occurring close to the hydrofoil tip. However, for the 2nd bending mode an equally response to the tip also occurs at the midspan of the hydrofoil. The boundary layer flow developing at the wall adjacent to the tip of the hydrofoil with its different inhomogeneous and anisotropic turbulence characteristics(mean flow, turbulence intensity and integral lengthscale) relative to those of the free stream, in conjunction with the fact that the maximum of the frequency response function appears at the tip of the hydrofoil, could have a major effect on the structural vibration response. The effects of inhomoegeneity and anisotropy will be incorporated into an enhanced model in the future.

4 CONCLUSIONS

The structural response of an elastic hydrofoil in a homogeneous isotropic turbulent flow has been studied in this paper. To achieve this, an analytical model implementing the correlation method has been combined with Sears' model of unsteady hydrodynamic gust and Theodorsen's theory for the lift and moment due to the heaving and pitching motion of a strip of the cantilevered hydrofoil motion.This method uses strip theory and requires the turbulence intensity and its integral length-scale as input for the characterization of the space-time correlation function of the turbulent velocity fluctuations assuming Taylor's frozen flow hypothesis for the convected vortices. The Euler-Bernoulli beam and the torsional equations have been used for the equations of motion. The model provided consistent agreement of the resonant frequencies in still air and water but overpredicted the hydrofoil vibration response at high frequencies under flow. Discrepancies between the analytical model and experimental measurements could have been due to uncertainties in material and geometrical properties as well as due to the confinement of the flow and the developing wall boundary layer adjacent to the hydrofoil tip which was not considered by the correlation method.

ACKNOWLEDGEMENTS

The authors would like to thank Dr. Richard Howell (Contractor to Defence, YTEK Pty Ltd) and Mr. Witold Waldman (Contractor to Defence, YTEK Pty Ltd) for discussions on unsteady aerodynamics.

REFERENCES

Blake, W.K. (1974).The radiation from free-free beams in air and in water. *Journal of Sound and Vibration*, vol. 33(4), pp. 427-450.
Blake, W.K. and Maga, L.J. (1975). On the flow-excited vibrations of cantilever struts in water. I. Flow-induced damping and vibrations. *The Journal of the Acoustical Society of America,* vol.57, No.3, pp.610-625.
Chae, E.J., Akcabay, D.T., Lelong, A., Astolfi, J.A. and Young, Y.L. (2016). Numerical and experimental investigation of natural flow-induced vibrations of flexible hydrofoils. *Phys. Fluids,* vol.28, 075102.
Dowell, E.H. (2015) A Modern Course in Aeroelasticity 5th ed., *Springer*.
Ducoin, A., Astolfi, J.A. and Sigrist, J.F. (2012). An experimental analysis of fluid structure interaction on a flexible hydrofoil in various flow regimes including cavitating flow. *European journal of Mechanics B/Fluids,* 36, pp. 63
Ducoin, A. and Young, Y.L. (2013). Hydroelastic response and stability of a hydrofoil in viscous flow. *Journal of Fluids and Structures,* 38, pp. 4-57.
D' Ubaldo, O., Ghelardi, S. and Rizzo C.(2021). FSI simulations for sailing yaght high performance appendages. *Ships and Offshore Structures*, vol.16, 2, pp.200-215.
Everstine, G.C. and Henderson, F.M. (1990). Coupled finite element/boundary element approach for fluid-structure interaction. *The Journal of the Acoustical Society of America*, vol.87, 5, pp.1938-1947.
Glegg, S. and Devenport, W. (2017). Aeroacoustics of low Mach number flows. 1st ed., *Academic Press.*
Houghton, E.L. and Carpenter, P.W. (2003) Aerodynamics for Engineering Students. 5th edition,*Butterworth-Heinemann.*
Jang, W., Hong, S., Song, J., Kwon, H. and Choi, W. (2020). Study on Vortex-Induced Vibration Predictions for Ship Rudders. *Journal of Ocean Engineering and Technology*, vol.34, 5, pp. 325-333.
Jiang C.W., Chang M.S. and Liu Y.N. (1991). The effect of turbulence ingestion on propeller broadband thrust. *DTRC/SHD Report ADA245326*, Bethesda, U.S.A, December 1991.
Lelong, A., Guiffant, P. and Astolfi, J.A. (2016). An experimental Analysis of the Structural Response of Flexible Lightweight Hydrofoils in Various Flow Conditions. *16th International Symposium on Transport Phenomena and Dynamics of Rotating Machinery*, Apr. 2016, Honolulu, United States, hal-01890079.
Lelong, A., Guiffant, P. and Astolfi, J.A. (2018). An experimental Analysis of Structural Response of Flexible Lightweight Hydrofoils in Cavitating Flow. *Journal of Fluids Engineering* , vol.140, 021116, pp.1-9.
Merz, S., Oberst, S., Dylejko, P.G., Kessissoglou, N.J., Tso, Y.K. and Marburg, S. (2007). Development of coupled FE/BE models to investigate the structural and acoustic responses of a submerged vessel. *Journal of Computational Acoustics*, Vol.15, No.1 , pp. 23-47.
Rao, S.S. (2007). Vibration of Continuous Systems. *John Wiley & Sons, Inc*, New Jersey, USA.
Sears, W.R. (1941) Some aspects of non-stationary airfoil theory and its practical application. *Journal of the Aeronautical Sciences*, vol.8 (3), pp. 104-108.
Sevik, M. (1974) Sound radiation from a subsonic rotor subjected to turbulence. Int. Symp. Fluid Mech. Des. Turbomach., Pennsylvania State University, University Park; NASA SP-304 Part II.
Theodorsen, T. (1935) General Theory of Aerodynamic Instability and the Mechanism of Flutter. *NACA report 496.*